

# Journal of Biomedical Optics

[SPIEDigitalLibrary.org/jbo](http://SPIEDigitalLibrary.org/jbo)

## **Practicability and safety of laser-assisted reduction surgery**

Yixin Wang  
Qiuyang Xiong  
Zhibin Ye  
Jianhong Ge



**SPIE**

# Practicability and safety of laser-assisted reduction surgery

Yixin Wang, Qiuyang Xiong, Zhibin Ye, and Jianhong Ge

Zhejiang University, The State Key Laboratory of Modern Optical Instrumentation, Hangzhou, Zhejiang 310027, China

**Abstract.** We have presented an innovative laser-assisted reduction surgery (LARS) based on plasma-induced ablation and photodisruption effects. In addition, we developed a laser operation system. Fetuses of mice from the Institute for Cancer Research that were immersed in physiological saline were irradiated by convergent-pulsed laser with a wavelength of 1064 nm, pulse width of 6 ns, and pulse energy of 50 mJ. The hearts of the postirradiated fetuses were significantly damaged, which resulted in rapid fetal death. We also substantiated the safety of LARS by analyzing the heat distribution of the induced laser pulse with thermal distribution equations. The results demonstrate that this innovative method for pregnancy reduction is feasible. © 2013 Society of Photo-Optical Instrumentation Engineers (SPIE) [DOI: 10.1117/1.JBO.18.11.118002]

Keywords: pulse laser; selective reduction; ablation; photodisruption.

Paper 130339RR received May 13, 2013; revised manuscript received Oct. 14, 2013; accepted for publication Oct. 22, 2013; published online Nov. 18, 2013.

## 1 Introduction

The prevalence of multifetal pregnancy has recently shown an exponential increase due to the wide use of ovarian stimulation fertility drugs and assisted reproductive technology. Although most *in vitro* fertilization centers reduce the dose of ovulation induction drugs and limit the number of embryos per transfer in order to reduce the incidence of multiple gestations, multiple pregnancies are still unavoidable. Multifetal pregnancy, especially with more than two embryos, has a high risk of obstetric and perinatal morbidity and mortality.<sup>1–3</sup> In addition, multifetal pregnancy significantly increases the risk of concomitant disease, such as gestational diabetes, abscess, intrauterine growth restriction, and twin-to-twin transfusion syndrome, for which selective reduction surgery is required.<sup>1–6</sup> Further, the risk of premature delivery and complications is closely related to the number of fetuses. The health status of both the gravida and the embryos should be monitored when more than three intrauterine embryos are present.<sup>3,7</sup>

Multifetal pregnancy reduction was introduced to avoid the increased incidence of abortion and premature labor associated with multiple gestations.<sup>8</sup> The main techniques of pregnancy reduction surgery currently in use include amniocentesis, potassium chloride injection by fetal abdominal puncture, formaldehyde injection into the fetal heart, fetoscopic air embolism, and transvaginal ultrasound-guided reduction.<sup>1,2,8–10</sup> However, these conventional techniques have many disadvantages, including long operative time, complicated surgeries, and risks of vessel perforation.<sup>11</sup> Consequently, a safer and more accurate operative technique is required.

In this study, we present a novel reduction method that used a 1064-nm pulsed laser to overcome these disadvantages of traditional surgery. Laser surgery allows the noncontact cutting and removal of a wide variety of living tissues.<sup>11–14</sup> Compared to the conventional pregnancy reduction surgery, laser technique can shorten the duration of surgery, avoid the deviation caused

by quickening, improve the accuracy of the operation, minimize the surgical trauma, and reduce the patient's recovery time. Moreover, laser beams can be conducted at distance by a flexible optical fiber that can be integrated with manipulators and robots.<sup>15–17</sup>

Five categories of interaction types are classified according to the laser energy density, including photochemical interaction, thermal interaction, photoablation, plasma-induced ablation, and photodisruption.<sup>18</sup> Laser-assisted reduction surgery (LARS) is based on plasma-induced ablation and photodisruption effects to achieve the ideal damage. Plasma-induced ablation is the result of plasma ionization during the laser pulse irradiation of the biological tissue. The damage range is spatially confined to the breakdown region. However, photodisruption can create much greater damage than plasma-induced ablation due to concomitant mechanical effects, such as shockwave and cavitation. Photodisruption is, therefore, the major cause of photoinduced damage in experimental conditions. The biological tissue is split by mechanical forces, shock wave, and cavitation effects during photodisruption.<sup>18,19</sup> Shock wave-induced tissue effects occur mainly on a cellular and subcellular level, whereas cavitation results in macroscopic tissue disruption. The mechanical effects observed in plasma-mediated laser surgery are dominated by cavitation.<sup>20,21</sup>

In this study, fetuses of mice from the Institute for Cancer Research (ICR) that were exposed to air and immersed in physiological saline were irradiated by a convergent 1064-nm pulsed laser. We used the stereomicroscope to observe and record fetal damage. We also attempted to substantiate the safety of LARS by analyzing the heat distribution of the induced pulse using thermal distribution equations.

## 2 Materials and Methods

### 2.1 Animal Model

Three pregnant female mice from the ICR were used as animal models, with a total of 60 white fetuses. The mouse fetuses were used to imitate human embryos in this experiment. Fetuses

Address all correspondence to: Jianhong Ge, Zhejiang University, The State Key Laboratory of Modern Optical Instrumentation, Hangzhou, Zhejiang 310027, China. Tel: 086-13516810806; Fax: 057188981976; E-mail: [jianhong@zju.edu.cn](mailto:jianhong@zju.edu.cn)

similar in size to the 2-month-old human embryo (~15-mm long and 8-mm wide) were adopted for our study.

## 2.2 Experiments with Near-Infrared Nanosecond Laser Pulses

The experimental setup is shown in Fig. 1. The Nd:YAG-pulse laser (Dawa-200, Beamtech Optronics Co., Ltd, Beijing, China) with a wavelength of 1064 nm and duration of 6 ns was used as the laser source used in the experiment. The repetition rates are adjustable between 1 and 10 Hz, and the intensity profile of the output laser beam is nearly Gaussian mode ( $TEM_{00}$ ). The wavelength of 1064 nm is optimally suited for clinical use due to the low absorption at the retina and the invisibility of the radiation, avoiding dazzling of the patient.<sup>14</sup> In addition, the 1064-nm pulsed laser has a low absorptivity in biological tissue and a penetration depth of ~4 to 6 mm, producing optimal successful biological tissue damage. The advent of compact and reliable ultrashort-pulsed laser has made very fine laser effects achievable, as the energy threshold for optical breakdown decreases with a reduction in pulse duration.<sup>19,22</sup> As a nanosecond pulse has a high probability of producing the effects of photo-disruption needed for LARS, we chose a 1064-nm, 6-ns pulsed laser for our experiments.

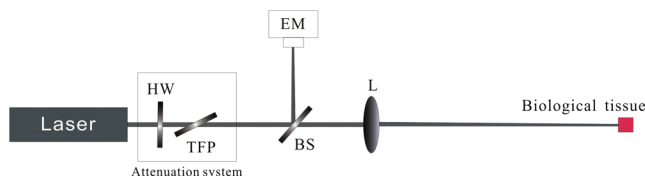


**Fig. 1** Experimental setup for selective reduction. HW: half wave plate; TFP: thin film polarizer; BS: beam splitter; EM: energy meter; L: spherical lens.

The attenuation system consisted of a half-wave plate, and a thin film polarizer was applied to adjust the irradiation energy to the fetus. The irradiation energy could be changed from 10 to 200 mJ. The laser beam was focused to a spot on the fetal chest ~400  $\mu\text{m}$  in size using a lens with a focal length of 750 mm. A charge coupled device camera was connected to the stereomicroscope (XTL-3400) to record images of fetal damage.

We chose a 50-mJ pulsed laser for the fetal irradiation experiments as a compromise taking both the ablation effect and the damage threshold of clinical optical fiber into consideration. The energy density of the 50-mJ pulse can reach  $10^{10}$  W/cm<sup>2</sup> in the ablation region when converged by the lens of 750-mm focal length.<sup>23,24</sup> The fetus was immersed in the physiological saline (0.154 mol/L NaCl solution) to imitate amniotic fluid clinically, as physiological saline has the same osmotic pressure as human plasma. The thickness of the physiological saline layer was 1 mm. The laser beam with a wavelength of 1064 nm was focused on the heart of the experimental fetus to penetrate the thoracic cavity and produce serious cardiac damage for embryo reduction.

## 3 Results and Discussion

### 3.1 Surface Morphology

Part of the skin, ribs, and lung was ablated, and a hole was created on the thoracic cavity as the laser irradiated the fetal thorax, making it possible to simultaneously observe the blood outflow from the injury. The fetus suffered cardiac arrest after a total of 30 laser pulses. The irradiated fetuses were then observed under the microscope, and we found that all the fetuses either died instantly or suffered cardiac arrest within 2 min. The results are shown in Fig. 2.

Figure 2(a) shows the entire fetus after laser irradiation and visualizes the blood outflow from the fetus. Figure 2(b) shows a clean cut and definite removal of tissue without the evidence of

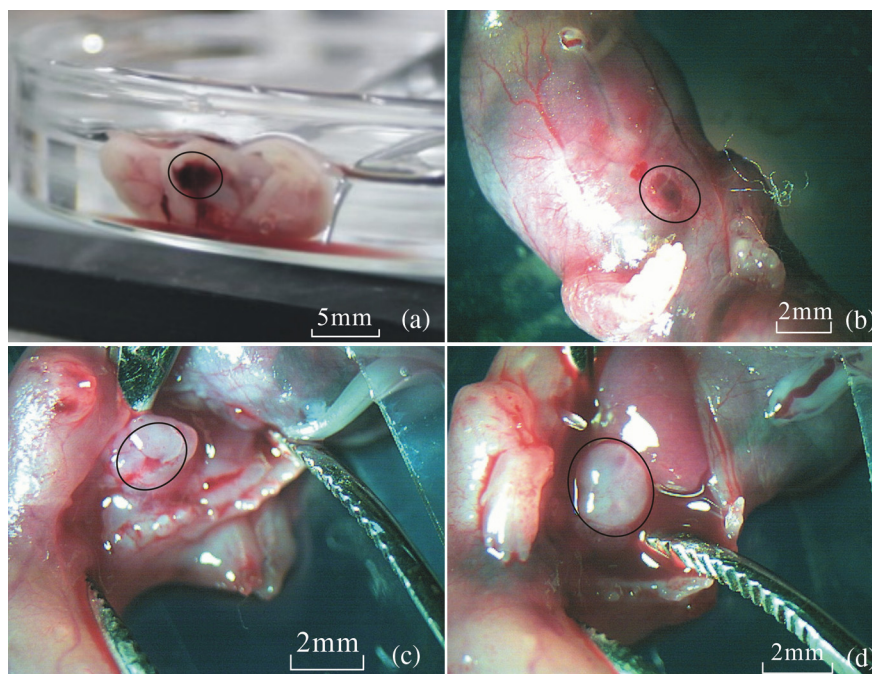


**Fig. 2** Images of the mouse fetuses. (a) Entire fetus irradiated by laser; (b) damaged part of the skin on the fetal chest; (c) damaged fetal heart irradiated with pulse laser; (d) complete fetal heart without any destruction. Damaged parts are marked by black circles.

thermal damage. Figure 2(c) shows a megascopic hole that was submillimeter in size on the fetal heart. The complete fetal heart is shown in Fig. 2(d) for comparison.

Prior to these experiments on fetuses, we used bovine muscle tissue as the experiment tissue to determine the most suitable laser parameters and the possibility of using LARS. We divided 48 samples of bovine muscle tissue into groups according to pulse energy and repetition rate.<sup>23,24</sup> The results suggested that the level of damage is proportional to the pulse energy and inversely proportional to the repetition rate. A higher repetition rate results in smoother and more regular lesions on the samples. The 10-Hz laser pulse can also shorten the operative time, reducing the possibility of quickening, and weakening the influence on other embryos. Very clean and well-defined removal of tissue without evidence of thermal damage can be achieved by choosing appropriate laser parameters.<sup>25</sup>

Compared with the former experiment results in air,<sup>23,24</sup> immersion in water increases the scale of the damage (Fig. 3).

The most important difference between ablation in air and in a liquid environment is that the liquid confines the movement of the ablation products.<sup>21</sup> In a liquid environment, the expansion of the hot vapor generated by the laser irradiation is inhibited.<sup>19</sup> The confining effect of the liquid results in considerably higher temperatures and pressures within the target than ablation in a gaseous environment for any given radiant exposure, because the expansion of the ablation products and the adiabatic cooling of the ablation products proceed more slowly.<sup>19,26</sup> A number of researchers have found that the potential for mechanical collateral damage in a liquid environment is much larger than that for ablation in air.<sup>18,21,27</sup> Plasma-mediated laser-material interaction in a liquid environment is disruptive due to the effective conversion of light energy into mechanical energy.<sup>19,22</sup> The conversion efficiency of light energy into mechanical energy during optical breakdown is large, reaching up to 90% at a 6-ns pulse

duration.<sup>28–31</sup> The laser energy is decreased due to absorption and scattering when the fetus is immersed in physiological saline. However, the confining effect of the liquid results in considerably higher pressure and a more effective transduction of the laser energy into mechanical energy,<sup>21,32,33</sup> which can lead to significant tissue damage.

### 3.2 Theoretical Calculations

Thermal effects are significant in most cases of laser surgery and must be avoided in LARS as well. In order to test the hypothesis that the thermal effect of a laser has only a negligible influence on the other embryos, we calculate the heat distribution created by the laser using the heat conduction equation. The internal heat source of the fetus and the heat exchange are negligible compared with the heat caused by laser incidence. To simplify the calculation, we regarded the heat source created by laser as a point and used a cube to simulate the fetus. The temperature distribution function  $u(x, y, z, t)$  meets the conditions of the following equations:<sup>34</sup>

$$\begin{cases} \frac{\partial u}{\partial t} = k^2 \left( \frac{\partial^2 u}{\partial x^2} + \frac{\partial^2 u}{\partial y^2} + \frac{\partial^2 u}{\partial z^2} \right) \\ u|_{x=0} = u|_{x=a} = 0 \\ u|_{y=0} = u|_{y=b} = 0 \\ u|_{z=0} = u|_{z=c} = 0, \quad (0 < x < a, 0 < y < b, 0 < z < c, t < 0). \end{cases} \quad (1)$$

Here,  $k$  is the thermal conductivity of biological tissue,  $k = 0.35 \text{ Wm}^{-1} \text{ K}^{-1}$ ;  $a$ ,  $b$ , and  $c$  are the length, width, and height of the mouse fetus ( $a = 0.015 \text{ m}$ ,  $b = c = 0.007 \text{ m}$ ). Increased temperature at the initial time is calculated by  $c = E / (m\Delta T)$ . For simplicity, the initial temperature is set as a rectangular distribution:

$$\phi(x, y, z) = \begin{cases} 200 & (0.007 < x < 0.0074, 0.003 < y < 0.0034, 0.001 < z < 0.0014) \\ 0 & \text{others} \end{cases}. \quad (2)$$

The solution is

$$\begin{aligned} u(x, y, z, t) = & \sum_{n=1}^{\infty} \sum_{m=1}^{\infty} \sum_{l=1}^{\infty} \frac{1600}{\pi^3 nml} \left[ \cos\left(\frac{7n\pi}{15}\right) - \cos\left(\frac{7.4n\pi}{15}\right) \right] \\ & \times \left[ \cos\left(\frac{3m\pi}{7}\right) - \cos\left(\frac{3.4m\pi}{7}\right) \right] \\ & \times \left[ \cos\left(\frac{l\pi}{7}\right) - \cos\left(\frac{1.4l\pi}{7}\right) \right] e^{-\left(\frac{n^2\pi^2}{a^2} + \frac{m^2\pi^2}{b^2} + \frac{l^2\pi^2}{c^2}\right)t} \\ & \times \sin\left(\frac{n\pi}{a}x\right) \sin\left(\frac{m\pi}{b}y\right) \sin\left(\frac{l\pi}{c}z\right). \quad (3) \end{aligned}$$

Figure 3 shows the temperature distribution of the  $xy$ -plane ( $z = 1 \text{ mm}$ ) at four different time points. The initial increased temperature is 450 K at the irradiation point [Fig. 4(a)]. According to the data shown in Figs. 4(b) and 4(c), we found that the space scale of the heat transmission was  $< 2 \text{ mm}$ , which is much smaller than the size of the embryo. Figure 4(d) shows that the heat has totally dissipated at  $t = 1 \text{ ms}$ . The thermal effect caused by 1 pulse does not exist at the arrival of the next pulse, indicating that there was no heat overlap of two

adjacent pulses. The results suggest that the embryo can be reduced without any thermal effect on the other embryos.

Then, we analyze the propagation distance and time of shock waves and cavitation. The amniotic fluid at the first 2 months of pregnancy is relatively pure, and its property is similar to water. Therefore, we calculate the distance and time by the parameters of water in the following analysis and calculation.

Laser-induced shock waves typically reach speeds of up to 5000 m/s at the very focus and eventually slow down to the speed of sound.<sup>35–37</sup> Only 1% to 5% of the incident pulse energy is converted to shock wave energy. The energies contained in shock waves are given by:<sup>38</sup>

$$E_s = (p_1 - p_0)A_s\Delta r, \quad (4)$$

with pressure inside the medium  $p_0$ , shock wave pressure  $p_1$ , shock wave surface area  $A_s$ , and shockwave width  $\Delta r$ .

The pressure decay is significantly steeper for those shock waves. The calculations for shock waves induced by nanosecond pulses were performed by Vogel et al.<sup>38</sup> Their results are the initial pressure at the boundary of the laser plasma was 21 kbar for 1 mJ-pulses with a duration of 6 ns, and in a distance of  $\sim 60 \mu\text{m}$  from the center of the shock wave emission, the

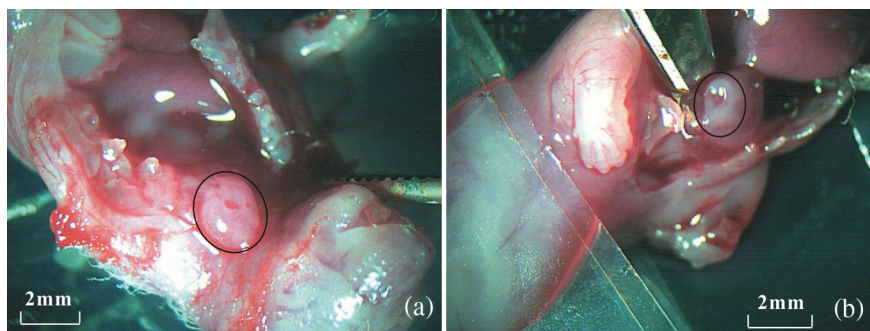


**Fig. 3** Images of the damaged fetal heart irradiated with pulsed laser. (a) Fetus exposed to air; (b) fetus immersed in physiological saline.

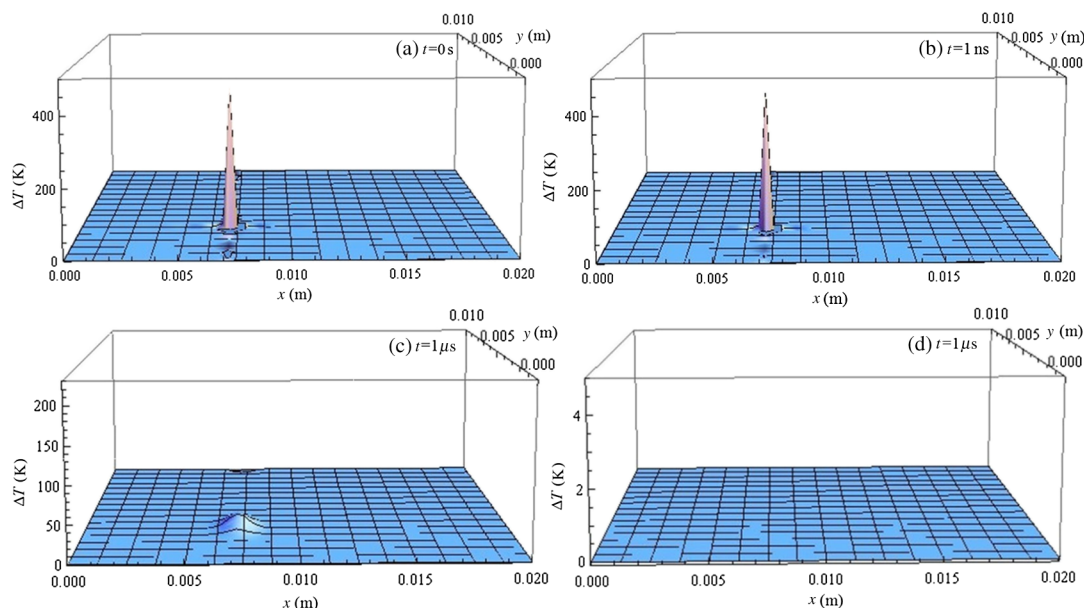


**Fig. 4** Temperature distribution of a  $xy$  cross section ( $z = 1$  mm) at four different time points. (a)  $t = 0$  s; (b)  $t = 1$  ns; (c)  $t = 1$   $\mu$ s; (d)  $t = 1$  ms.

pressure has already dropped to 10 kbar (normal atmospheric pressure) when applying 6-ns pulses.

Accordingly, we can calculate that when the shock wave propagates 3 mm, the pressure of shock decay to 10 kbar for 50-mJ pulse energy according to Vogel et al.<sup>38</sup> and Eq. (4). Consequently, the time for pressure drop to 10 kbar is on the microsecond level.

Laser-induced cavitations occur if plasmas are generated inside soft tissues or fluids.<sup>25</sup> By means of the high plasma temperature, the focal volume is vaporized. Vogel et al.<sup>39</sup> observed that the average energy loss of the cavitation bubbles during their first cycle is  $\sim 84\%$ , and the duration of first cycle is on the microsecond level. The major part of this loss is attributed to the emission of sound.

The bubble energy  $E_b$  by means of

$$E_b = 0.75\pi(p_{\text{stat}} - p_{\text{vap}})r_{\text{max}}^3, \quad (5)$$

where  $r_{\text{max}}$  is the maximum radius of cavitation,  $p_{\text{stat}}$  is the static pressure, and  $p_{\text{vap}}$  is the vapor pressure of the fluid.<sup>40</sup> This equation states that the bubble energy is given by the product of its maximum volume and the corresponding pressure gradient.

The data about maximum radius of cavitation bubble is provided according to the research work of Zysset et al.<sup>41</sup> The

radius of cavitation bubble is not relate to the pulse duration for picosecond and nanosecond pulses, and 1-mJ pulsed energy is corresponding to a 0.7-mm cavitation bubble in water. Cavitations were induced in water by a Nd:YAG laser. Therefore, we can obtain that the radius of cavitation bubble is 2.5 mm for 50 mJ, 6-ns laser pulse with Eq. (5).

The pressure of shock wave decay is significantly quick. The pressure decay to normal atmospheric pressure for 50 mJ, 6-ns pulse energy while the shock wave propagated 3 mm. Laser-induced cavitations are generated at the focal point of laser

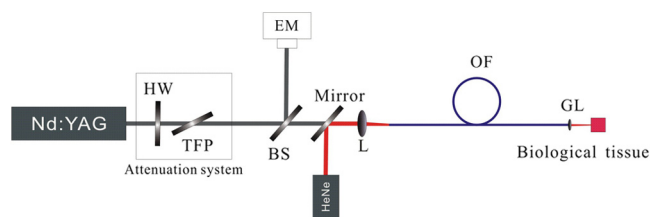


**Fig. 5** Experimental setup for selective reduction in the subsequent experiments. HW: half wave plate; TFP: thin film polarizer; BS: beam splitter; EM: energy meter; Mirror: 1064-nm high transmittance and 632-nm high reflectivity; L: spherical lens; OF: optical fiber; GL: grin lens.

pulse and the range of oscillations is 2.5 mm for 50-mJ laser pulse. These results suggest that the embryo can be reduced without shock wave and cavitation effect on the other embryos. Even though the site of break-down is not inside but outside the target fetus due to improper aiming, the embryos can be not affected by the laser pulse.

## 4 Conclusions and Outlook

### 4.1 Conclusions

In conclusion, we explored fetus ablation using the nanosecond 1064-nm laser pulse. We found that the fetus dies within 2 min after 30 Nd:YAG laser pulse irradiation. The laser pulse causes fatal damage to the embryo without affecting other embryos when the pulse energy is used appropriately. The results confirm the feasibility, practicability, and safety of LARS for use in multifetal pregnancy reduction surgery. The results and analyses all show that LARS has several advantages over the conventional methods. Future studies using high-damage threshold optical fiber for transmitting the pulsed laser energy in clinical operations are required.

### 4.2 Outlook

In the subsequent experiments, we will use the optical fiber to transmit the laser beams, which can be conducted at a distance by a flexible optical fiber that can be integrated with manipulators and robots. The 1064-nm laser beams can be transmitted in quartz optical fiber and the optical fiber can be a transvaginal point to the fetus with He-Ne laser as a visible light direction and endoscopes. These reasons can ensure that the laser is focused at the fetus's heart precisely. This setup for selective reduction surgery (Fig. 5) can be made with the laser focusing at the fetus's heart accurately. Now, we are trying our best to find high-threshold optical fiber to insure the reproducibility of our technology.

## References

- R. T. Mansour et al., "Multifetal pregnancy reduction: modification of the technique and analysis of the outcome," *Fertil. Steril.* **71**(2), 380–384 (1999).
- G. Iberico et al., "Embryo reduction of multifetal pregnancies following assisted reproduction treatment: a modification of the transvaginal ultrasound-guided technique," *Hum. Reprod.* **15**(10), 2228–2233 (2000).
- O. Torok et al., "Multifetal pregnancy reduction is not associated with an increased risk of intrauterine growth restriction, except for very-high-order multiples," *Am. J. Obstet. Gynecol.* **179**(1), 221–225 (1998).
- V. L. Miller et al., "Multifetal pregnancy reduction: perinatal and fiscal outcomes," *Am. J. Obstet. Gynecol.* **182**(6), 1575–1580 (2000).
- S. J. Fasouliotis and J. G. Schenker, "Multifetal pregnancy reduction: a review of the world results for the period 1993–1996," *Eur. J. Obstet. Gynecol. Reprod. Biol.* **75**(2), 183–190 (1997).
- A. Sutcliffe et al., "Outcome for children born after in utero laser ablation therapy for severe twin-to-twin transfusion syndrome," *Br. J. Obstet. Gynaecol.* **108**(12), 1246–1250 (2001).
- M. A. Ormont and P. A. Shapiro, "Multifetal pregnancy reduction: a review of an evolving technology and its psychosocial implications," *Psychosomatics: J. Consult. Liaison Psychiatry* **36**(6), 522–530 (1995).
- H. Kanhai et al., "Selective termination in quintuplet pregnancy during first trimester," *The Lancet* **327**(8495), 1447–1449 (1986).
- E.-M. Chang et al., "A case of successful selective abortion using radio-frequency ablation in twin pregnancy suffering from severe twin to twin transfusion syndrome," *J. Korean Med. Sci.* **24**(3), 513–516 (2009).
- M. S. Coffler et al., "Early transvaginal embryo aspiration: a safer method for selective reduction in high order multiple gestations," *Hum. Reprod.* **14**(7), 1875–1878 (1999).
- K. O'Donoghue et al., "Interstitial laser therapy for fetal reduction in monochorionic multiple pregnancy: loss rate and association with aplasia cutis congenita," *Prenatal Diagn.* **28**(6), 535–543 (2008).
- L. T. Canguero et al., "Femtosecond laser ablation of bovine cortical bone," *J. Biomed. Opt.* **17**(12), 125005 (2012).
- A. Vogel et al., "Femtosecond-laser-induced nanocavitation in water: implications for optical breakdown threshold and cell surgery," *Phys. Rev. Lett.* **100**(3), 038102 (2008).
- J. Umanzor-Alvarez et al., "Near-infrared laser delivery of nanoparticles to developing embryos: A study of efficacy and viability," *Biotechnol. J.* **6**(5), 519–524 (2011).
- X. Wang, C. Zhang, and K. Matsumoto, "In vivo study of the healing processes that occur in the jaws of rabbits following perforation by an Er, Cr: YSGG laser," *Lasers Med. Sci.* **20**(1), 21–27 (2005).
- S. R. Visuri, J. T. Walsh, and H. A. Wigdor, "Erbium laser ablation of dental hard tissue: effect of water cooling," *Lasers Surg. Med.* **18**(3), 294–300 (1996).
- M. Sivakumar et al., "Sealing of human dentinal tubules by KrF 248 nm laser radiation," *J. Laser Appl.* **18**(4), 330–333 (2006).
- A. Vogel and V. Venugopalan, "Mechanisms of pulsed laser ablation of biological tissues," *Chem. Rev.* **103**(2), 577–644 (2003).
- A. Vogel et al., "Energy balance of optical breakdown in water at nanosecond to femtosecond time scales," *Appl. Phys. B: Lasers Opt.* **68**(2), 271–280 (1999).
- P. P. Banerjee, "Principles of Nonlinear Optics," *DTIC Document* (1989).
- A. Vogel, S. Busch, and U. Parlitz, "Shock wave emission and cavitation bubble generation by picosecond and nanosecond optical breakdown in water," *J. Acoust. Soc. Am.* **100**(1), 148–151 (1996).
- A. Vogel et al., "Plasma formation in water by picosecond and nanosecond Nd: YAG laser pulses. I. Optical breakdown at threshold and superthreshold irradiance," *IEEE J. Sel. Top. Quantum Electron.* **2**(4), 847–860 (1996).
- J. H. Ge et al., "Experiment study of selective abortion surgery with 1064 nm pulsed laser," *Laser Optoelectron. Prog.* **49**(7), 138–141 (2012).
- J. H. Ge et al., "The research of photodisruption effect of biological tissues acted by high-power laser," *Acta Laser Biol. Sin.* **21**(2), 113–117 (2012).
- M. H. Niemz, *Laser-Tissue Interactions: Fundamentals and Applications*, Springer, Berlin, Heidelberg, New York (2007).
- D. Albagli et al., "Photomechanical basis of laser ablation of biological tissue," *Opt. Lett.* **19**(21), 1684–1686 (1994).
- E.-A. Brujan et al., "Dynamics of laser-induced cavitation bubbles near elastic boundaries: influence of the elastic modulus," *J. Fluid Mech.* **433**, 283–314 (2001).
- E. Brujan, T. Ikeda, and Y. Matsumoto, "Jet formation and shock wave emission during collapse of ultrasound-induced cavitation bubbles and their role in the therapeutic applications of high-intensity focused ultrasound," *Phys. Med. Biol.* **50**(20), 4797–4809 (2005).
- P. K. Kennedy, "A first-order model for computation of laser-induced breakdown thresholds in ocular and aqueous media. I. Theory," *IEEE J. Quantum Electron.* **31**(12), 2241–2249 (1995).
- P. K. Kennedy et al., "A first-order model for computation of laser-induced breakdown thresholds in ocular and aqueous media. II. Comparison to experiment," *IEEE J. Quantum Electron.* **31**(12), 2250–2257 (1995).
- E. J. Chapyak, R. P. Godwin, and A. Vogel, "A comparison of numerical simulations and laboratory studies of shock waves and cavitation bubble growth produced by optical breakdown in water," *Proc. SPIE* **2975**, 335–342 (1997).
- E.-A. Brujan et al., "Dynamics of laser-induced cavitation bubbles near an elastic boundary," *J. Fluid Mech.* **433**(1), 251–281 (2001).
- D. M. Harris and D. Fried, "Pulsed Nd: YAG laser selective ablation of surface enamel caries: I. Photoacoustic response and FTIR spectroscopy," *Proc. SPIE*, **3910**, 164–170 (2000).
- W. E. Schiesser and G. W. Griffiths, *A Compendium of Partial Differential Equation Models*, Cambridge University Press, New York, NY (2009).
- M. Felix and A. Ellis, "Laser-induced liquid breakdown—a step-by-step account," *Appl. Phys. Lett.* **19**(11), 484–486 (1971).

36. E. Carome, C. Moeller, and N. Clark, "Intense ruby-laser-induced acoustic impulses in liquids," *J. Acoust. Soc. Am.* **40**(6), 1462–1466 (1966).
37. C. Bell and J. Landt, "Laser-induced high-pressure shock waves in water," *Appl. Phys. Lett.* **10**(2), 46–48 (1967).
38. A. Vogel et al., "Mechanisms of intraocular photodisruption with picosecond and nanosecond laser pulses," *Lasers Surg. Med.* **15**(1), 32–43 (1994).
39. A. Vogel, W. Lauterborn, and R. Timm, "Optical and acoustic investigations of the dynamics of laser-produced cavitation bubbles near a solid boundary," *J. Fluid Mech.* **206**, 299–338 (1989).
40. L. Rayleigh, "On the pressure developed in a liquid during the collapse of a spherical cavity," *London, Edinburgh Dublin Philos. Mag. J. Sci.* **34**(200), 94–98 (1917).
41. B. Zysset, J. Fujimoto, and T. Deutsch, "Time-resolved measurements of picosecond optical breakdown," *Appl. Phys. B* **48**(2), 139–147 (1989).